CXCR4 enhances the inhibitory effects of bone mesenchymal stem cells on lung cell apoptosis in a rat model of smoking-induced COPD

JIANSHENG GAO
First Affiliated Hospital of Guangdong Pharmaceutical University
YULI LIANG
First Affiliated Hospital of Guangdong Pharmaceutical University
JIABAO CHEN
First Affiliated Hospital of Guangdong Pharmaceutical University
HUIHUI SHEN
First Affiliated Hospital of Guangdong Pharmaceutical University
HUA LIU (liuhuagy63@163.com)
First Affiliated Hospital of Guangdong Pharmaceutical University

Research Article

Keywords: CXCR4, Bone marrow mesenchymal stem cells, Chronic obstructive pulmonary disease, Antiapoptosis

Posted Date: August 11th, 2022

DOI: https://doi.org/10.21203/rs.3.rs-1910750/v1

Additional Declarations: No competing interests reported.

Version of Record: A version of this preprint was published at Apoptosis on January 31st, 2023. See the published version at https://doi.org/10.1007/s10495-022-01800-6.

Abstract

Objective

Chronic obstructive pulmonary disease (COPD) is the 3rd leading cause of death worldwide, and treatments are unsatisfactory, resulting in a major economic burden. Cellular therapy is commonly used for lung disease. We investigated treatment with CXCR4-overexpressing BMSCs during COPD model establishment.

Methods

We extracted and purified BMSCs from SD rats. Apoptosis induced by COPD was established by cigarette smoke exposure. BMSCs were transplanted in vivo twice a month during model establishment, and alveolar rupture in the lung was assessed. Lung cell apoptosis was assessed by TUNEL analysis, and the concentrations of apoptotic proteins in the lungs were detected by Western blotting.

Results

We successfully isolated BMSCs and established CXCR4-overexpressing BMSCs. Continuous cigarette smoke exposure caused alveolar septal rupture: in the model group, the 1-month alveolar MLI was significantly lower than that at the third month ($p < 0.05$). In the third month, the alveolar MLIs of the control and CXCR4-BMSC groups were lower than those of the model group (control group $p < 0.01$, CXCR4-BMSC group $p < 0.05$), and as shown by TUNEL staining, the apoptosis rates of the control and CXCR4-BMSC groups were significantly lower than those of the model groups ($p < 0.01$). The levels of the apoptotic proteins cleaved caspase-8, cleaved caspase-3 and cleaved PARP-1 were higher in the model group than in the control group ($p < 0.05$) and significantly lower in the CXCR4-BMSC group than in the model group ($p < 0.05$).

Conclusion

Transplantation of CXCR4-overexpressing BMSCs during COPD model generation significantly inhibited apoptosis via the extrinsic apoptosis pathway.

1. Introduction

Chronic obstructive pulmonary disease (COPD) is mostly caused by smoking, which leads to the destruction of alveolar septa and the formation of emphysema through the inflammatory response, oxidative stress, apoptosis and other pathways[1]. Apoptosis is one of the main pathogenic pathways of COPD and is involved in the complete pathogenesis of COPD. Recent studies have shown that apoptosis is significantly increased in the lung tissue of COPD patients, and DNA fragmentation is the main cause

of apoptosis[2][3]. In addition, animal experiments have shown that the formation of emphysema in a COPD model generated by exposure to cigarette smoke is related to cell apoptosis[4]. Clinical and basic trials have investigated antiapoptotic therapy for COPD[5][6][7]. Alveolar cell apoptosis in COPD patients was found to continue even after smoking cessation[8][9]; thus, antiapoptotic therapy during the development of COPD is particularly important. For more effective treatment of COPD or delayed progression of COPD, further antiapoptotic research should be performed.

The mortality rate of COPD is increasing yearly as the current therapies merely ameliorate the symptoms and cannot effectively delay disease progression[10][11][12]. Improving respiratory function by inhibiting cell apoptosis or repairing damaged lung tissue has become a major research direction, resulting in a focus on the transplantation of bone marrow mesenchymal stem cells (BMSCs) in vivo. BMSCs are cells of nonhematopoietic origin with the ability to differentiate into multiple cell types and repair tissue[13]. Due to their low immunogenicity and immunoregulatory ability, BMSCs have been extensively used for in vivo transplantation into COPD models to explore their therapeutic effects[14]. The majority of research findings indicate that MSCs can treat diseases via anti-inflammatory effects by promoting tissue repair and regeneration and through antioxidative, antiapoptotic and immunomodulatory activities[15][16][17] [18][19] [20][21]. Some studies have shown that MSCs can inhibit apoptosis by reducing the expression of apoptotic proteins in tissue and secreting vascular endothelial growth factor[22].

The apoptotic pathways in cells are complex, and the main apoptotic pathways include endogenous and exogenous apoptotic pathways[23][24]. Further research and exploration are needed to determine the antiapoptotic effects of BMSCs in COPD to delay the progression of this disease. A high concentration of SDF-1 can be detected in damaged organs, and BMSCs can be recruited and exert a therapeutic effect on damaged organs through the SDF-1 concentration gradient[25][26]. CXC chemokine receptor 4 (CXCR4) is the cognate receptor of SDF-1, and BMSCs that overexpress CXCR4 can more effectively home to the damaged tissue in vivo. Moreover, some studies have indicated that CXCR4 protein overexpression can enhance the paracrine effects of BMSCs[27][28][29][30].

In this study, a retrovirus transfection method was used to establish a CXCR4 overexpression model of BMSCs[31]. BMSCs were transplanted into in vivo rat models of COPD established by exposure to cigarette smoke[32][33]. Most studies have explored the intervention effect of some measures after the construction of animal models. The aim of the present study was to determine whether BMSCs inhibit lung cell apoptosis during the establishment of a rat model of COPD by exposure to cigarette smoke. Moreover, we investigated whether BMSCs could inhibit apoptosis in lung tissues and protect lung tissue from cigarette smoking-induced destruction by reducing the expression of cleaved caspase-3 through exogenous pathways and whether BMSCs overexpressing CXCR4 protein could more effectively inhibit cell apoptosis via the exogenous apoptotic pathway.

2. Methods

2.1 Experimental design

The trial design and study flow are shown in Fig. 1.

2.2 Ethics statement (animal)

This experiment was approved by the Ethics Committee of the First Affiliated Hospital of Guangdong Pharmaceutical University, Guangzhou, China. The animals for this experiment were specific pathogen-free (SPF) Sprague-Dawley (SD) rats purchased from Guangdong Medical Laboratory Animal Center.

2.3. Isolation and identification of BMSCs

Briefly, the hindlimbs were removed, and BMSCs were collected by flushing the marrow cavities with DMEM/F12 medium with 10% FBS and 1% penicillin–streptomycin. The whole bone marrow adherent method was used for the culture and isolation of primary BMSCs. BMSCs from the 3rd to 4th passages were identified by their morphologic and immunophenotypic characteristics and differentiation ability.

Differentiation medium (Cyagen Biosciences, Guangzhou, China) was used to induce BMSCs to differentiate into osteoblasts, adipocytes and chondrocytes. For the induction of osteogenic and adipogenic differentiation, BMSCs were seeded onto six-well plates (Corning, Corning, NY, USA) at a density of 2.0×10^4 cells per well and cultured with BMSC Osteogenic Differentiation Basal Medium and Adipogenic Differentiation Basal Medium. For induction of chondrogenic differentiation, 2.0×10^4 cells were pelleted in Chondro-Pelle and cultured in chondrogenic differentiation media. According to the instructions, BMSCs were cultured in differentiation media for 2–3 weeks, and the medium was refreshed every 3 days. At the end of the predetermined culture time, the results of osteogenic, adipogenic, and chondrogenic differentiation were determined by Alizarin red staining, Oil red O staining and Alcian blue staining, respectively.

The surface markers (CD90, CD29, CD34, CD45) of BMSCs were detected by flow cytometry. BMSCs were detached from T25 cell culture bottles (Corning, Corning, NY, USA) by trypsin and counted to adjust the initial cell density to 1×10^6 cells/mL with DMEM/F12 medium with 10% fetal bovine serum (FBS) and 1% penicillin-streptomycin. The cells were added to an Eppendorf tube at 1×10^6 cells/tube and incubated in the dark for 30 min at 4°C with the following monoclonal antibodies: CD90 antibody-FITC (EBioscience, USA), CD29 antibody-FITC (BioLegend, USA), CD34 antibody-PE (Santa, USA), CD45 antibody-PE (EBioscience, USA) and isotype controls for FITC and PE (both from BioLegend and Santa). After 30 min, the cells were washed three times with PBS and resuspended in 500 μL of PBS. A FACSCalibur system (BD Bioscience) was used to collect the BMSCs and analyze the expression of surface markers of BMSCs.

2.4 Establishment of stable CXCR4-overexpressing BMSCs

The sequence of rat CXCR4 (accession no. NM_022205.3) was obtained from the GenBank database. We designed cloning primers based on the rat CXCR4 sequence as follows: forward, 5'-CACAGAATTCATGGAAATATACACTTCG-3'; reverse, 5'-CACAGTCGACTTAGCTGGAGTGAAAACTT-3'. The CXCR4 sequence was collected after RT-PCR amplification and cloned into the pBABE-puro plasmid using the EcoRI and SalI restriction enzyme sites. The ligation mixture was transformed into competent Trans5α cells (Transgen Biotech, USA) to generate the recombinant plasmid. Plasmid DNA was extracted from Trans5α cells, and sequence analysis confirmed that the inserted sequences were the same as the sequence of rat CXCR4 obtained from the GenBank database. For stable overexpression, a mixture of X-tremeGENE (Roche, USA) with the plasmid at a ratio of 1:3 was added to Dulbecco's modified Eagle's medium (DMEM) and added to 6-well plates for the transfection of Platinum-E (Plat-E) packaging cells with the retroviral packaging vector pBABE-puro-CXCR4 or pBABE-puro-null.

Eight hours after cotransfection, the fresh medium was exchanged, and the recombinant retroviral vectors were harvested after culture for 48 h. Cell debris was removed by filtration. Third-passage BMSCs were seeded in 6-well plates and transduced with the negative control retroviral vector pBABE-puro-null or the overexpressing retroviral vector pBABE-puro-CXCR4. The confluence of BMSCs before transduction was lower than 60%. The retroviral vector and DMEM were mixed with polybrene at a ratio of 3:7 (Sigma-Aldrich, St. Louis, MO, USA) to obtain a final concentration of 4 ng/mL. After 8 h, the medium was replaced with DMEM, and the cells were cultured for 48 h. Subsequently, stably transfected cells were selected using culture medium containing puromycin (0.1 μg/μL).

2.5 Reverse transcription and real-time quantitative PCR (qRT-PCR)

qRT-PCR was used to detect and compare the mRNA expression of CXCR4 between CXCR4-BMSCs and pBABE-BMSCs. PCR was performed with 5'-CCACAGAGTCAGAATCCTCAAG-3' and 5'-GGTCAGTCTTTTAT ATCTGG GAAATG-3' as the forward and reverse primers, respectively. The total RNA of the BMSCs was extracted using TRIzol reagent, and Genomic DNA Eraser was used for the removal of genomic DNA. According to the manufacturer's instructions, a reverse transcription kit (TaKaRa, Japan) was used to transcribe the cDNA, and the SuperReal PreMix Plus SYBR GREEN kit (TaKaRa, Japan) was utilized for real-time qRT-PCR with the following program: 95°C for 30 sec, 40 cycles of 95°C for 10 sec, 60°C for 1 min, and 72°C for 30 sec, 95°C for 1 min, 60°C for 30 sec, and 95°C for 30 sec. After normalization with the internal control 18S, the $2^{-}\Delta\Delta Cq$ method was used to compare the CXCR4 mRNA expression levels between CXCR4-treated BMSCs exposed to cigarette smoke and pBABE-treated BMSCs exposed to cigarette smoke.

2.6 Establishment of the COPD rat model and cell therapy

A total of 64 healthy male SD rats (aged 3–4 weeks) were randomly divided into four groups (16 SD rats in each group): the control group, CXCR4-BMSC treatment + cigarette smoke exposure group (CXCR4-BMSC group), pBABE-BMSC treatment + cigarette smoke exposure group (pBABE-BMSC group) and COPD model group (model group). We used the cigarette smoke exposure method for the construction of the COPD rat models in this study. Animals in all of the groups with the exception of the normal group were exposed to commercially available cigarette smoke. As the experimental design showed, the rats in the CXCR4-BMSC, pBABE-BMSC and model groups were exposed to smoke from ten cigarettes (Coconut Tree brand, tobacco tar: 11 mg; nicotine smoke: 1.0 mg; flue gas of carbon monoxide: 13 mg) for 30 min/d (two sets of 5 cigarettes burned for approximately 15 min).

BMSCs were transplanted in vivo during the construction of the COPD rat models. As shown in the experimental design, BMSCs were intravenously injected twice a month. All intravenous injections were administered via the tail vein as follows: (1) CXCR4-BMSC group (injected via the tail vein with 1 mL of PBS containing 1×10^6 CXCR4-overexpressing BMSCs) and (2) pBABE-BMSCs group (injected via the tail vein with 1 mL of PBS containing 1×10^6 pBABE-puro-null-BMSCs). The animals in the control and model groups received injections of 1 mL of PBS via the tail vein.

2.7 Lung tissue harvesting

Six rats from each group were anesthetized with 3% pentobarbital sodium (0.3 mL/100 g) administered intraperitoneally, and the rats were fixed on a foam board to harvest lung tissue every month. The lung tissues were removed from SD rats and flushed with 10 mL of cold PBS to remove excess blood. The lower lobe of the right lung tissues was fixed with paraformaldehyde (4%), and the other lung tissues were snap-frozen in liquid nitrogen and stored at -80°C until use.

2.8 Hematoxylin and eosin (H&E) staining and measurement of the alveolar mean linear intercept (MLI)

The lung tissues were fixed with paraformaldehyde (4%) for 12 h and embedded in paraffin. A rotary slicer was used to slice the lung tissue into 5-μm-thick sections, and the sections were then stained with H&E. After H&E staining, the morphology of the lung tissue was observed and randomly photographed at 200× magnification under a light microscope, and the resulting photographs were used to measure the alveolar MLI excluding the sections of bronchi, large bronchioli and blood vessels. Image-Pro Plus 6.0 software was used to measure the alveolar MLI. First, seven horizontal and eleven vertical lines were drawn on each photograph. Second, the number of alveolar septa on each line was counted. Third, the following equation was used to measure the alveolar MLI, which was calculated by dividing the length of the grid line by the number of intersections with alveolar walls.

2.9 Western blotting

The expression of apoptotic proteins in the lung tissue of each group and the CXCR4 protein expression in BMSCs were detected by Western blotting. Total proteins from BMSCs and lung tissue were collected by lysis in RIPA lysis buffer containing a proteinase inhibitor. After a 30-min ice bath, the extracts were centrifuged at 12000 x g and 4°C for 30 min, and the supernatants were collected. After the protein concentration was measured by the BCA assay, the protein sample was mixed with SDS buffer at a ratio of 4:1 and boiled for 10 min. The proteins were separated by 12% SDS-PAGE and transferred to polyvinylidene fluoride (PVDF) membranes, and the PVDF membranes were blocked in TBST containing 5% nonfat milk at room temperature for 2 h and washed three times with TBST. Subsequently, the PVDF membranes were incubated with the following primary antibodies overnight: rabbit anti-rat CXCR4 (Abcam, 1:100), mouse anti-rat GADPH (Abcam, 1:1000), rabbit anti-rat cleaved caspase-8 (Abcam, 1:1000), rabbit anti-rat cleaved caspase-3 (Abcam, 1:1000), rabbit anti-rat cleaved PARP-1 (Abcam, 1:1000), and rabbit anti-rat cleaved PARP-β-actin (Abcam, 1:1000). The PVDF membranes were washed three times with TBST and incubated with HRP-conjugated secondary antibodies (1:5000) for 2 h. A chemiluminescent detection system (Bio-Rad, USA) was used to detect the target protein, and the gray value was measured using ImageJ software.

2.10 Terminal deoxynucleotidyl transferase biotin-dUTP nick end labeling (TUNEL) assay

TUNEL staining was used to detect the apoptotic signal of lung cells. The lung tissue sections were incubated with proteinase K for 25 min at 37°C and washed three times with PBS. After permeabilization with Triton X-100 for 20 min, the lung sections were incubated with a reaction mixture that contained TdT and dUTP (mixed at a ratio of 1:9) for 30 min at 37°C. The sections were treated for 10 min in 3% hydrogen peroxide to quench endogenous peroxidase activity, incubated with Converter-POD solution, washed with PBS and stained with DAB. The cells were randomly photographed at 200× magnification under a light microscope. The number of TUNEL-positive cells was counted using Mage-Pro Plus 6.0 software, and fields containing bronchi or large bronchioles were excluded from the analysis.

Statistical analysis

Statistical analyses were performed using SPSS 17.0 Statistical Analysis Software. All the data were tested for normality using the Shapiro-Wilk test. The data all showed a normal distribution and are expressed as the means ± SDs. Student's t test was used to examine the significance of the differences between two groups, and $p < 0.05$ was considered to indicate statistical significance.

3. Results

3.1 Morphological observations and induction of differentiation

The results confirmed that the 3rd -passage cultured cells were BMSCs (Fig. 2). Microscopically, the BMSCs exhibited a typical spindle shape and displayed a vortex shape once they reached 80–90% confluence (Fig. 2-A). After induction with differentiation medium, the mineralization capacity of the osteoblasts was assessed by Alizarin red staining, and the bone-like nodules were stained red by Alizarin red (Fig. 2-B). The adipogenic differentiation of BMSCs was demonstrated by red oil drops after oil red O staining (Fig. 2-B). BMSCs could be differentiated into chondrogenic-like cells, and proteoglycans were stained blue by Alcian blue (Fig. 2-B). Flow cytometric analysis of the surface markers of BMSCs showed that the positive rates of CD29 and CD90 were 97% and 97%, respectively, and the positive rates of the isotype control were 0.51% and 0.51%, respectively; the positive rates of CD45 and CD34 were 0.42% and 0.42%, respectively, and the positive rates of the isotype control were 0.51% and 0.51%, respectively (Fig. 2-C).

3.2 Overexpression of CXCR4 mRNA and protein in BMSCs

The CXCR4 mRNA and protein expression in BMSCs after transfection was analyzed by qRT-PCR and Western blotting. The qRT-PCR results indicated that the CXCR4 mRNA level in the CXCR4-BMSCs was significantly higher than that in the pBABE-BMSCs, and the difference between the two groups was significant ($p < 0.001$, Fig. 3-A). Western blotting detection of CXCR4 protein expression in the transfected BMSCs showed that the CXCR4-BMSCs exhibited significantly higher CXCR4 expression than the pBABE-BMSCs ($p < 0.01$, Fig. 3-B).

3.3 CXCR4-BMSC transplantation effectively reduced the destruction of alveoli

HE staining revealed that exposure to cigarette smoke induced alveolar septal rupture, and the alveolar MLI gradually increased as the exposure time to cigarette smoke increased. A statistical analysis indicated that the MLI in the third month (59.8750 ± 8.2148) was clearly higher than that in the first month (39.1049 ± 3.0874), and the difference was significant ($p < 0.05$, Fig. 4-B). The comparison of the between-group differences in the third month revealed that the MLIs of the control group (34.4288 ± 1.5973) and the CXCR4-BMSC group (40.21932 ± 2.0722) were lower than that of the model group (59.8750 ± 8.2148), and the differences were significant (control group vs. model group, $p < 0.01$; CXCR4-BMSC group vs. model group, $p < 0.05$). The alveolar MLI of the pBABE-BMSC group was also lower than that of the model group, but the difference between these groups was not significant ($p > 0.05$, Fig. 4-B).

3.4 Treatment with BMSCs overexpressing CXCR4 significantly reduced TUNEL staining in lung tissue

Cell apoptosis in lung tissue collected in the third month was assessed by TUNEL analysis, and positive staining, which appeared tan or brown, was located in the nucleus (Fig. 5-A). The apoptotic index of the model group was significantly higher than that of the control group ($p < 0.01$). In addition, transplanted BMSCs in vivo reduced the apoptotic index of lung tissue. The apoptotic index of the lung tissue collected from the CXCR4-BMSC group was significantly lower than that of the lung tissue collected from the model group ($p < 0.01$). The apoptotic index of the lung tissue collected from the pBABE-BMSC group was also lower than that of lung tissue collected from the model group ($p < 0.05$, Fig. 5-B).

The transplantation of BMSCs overexpressing CXCR4 effectively decreased the expression of apoptotic proteins in lung tissue

A significant difference in the expression of apoptotic proteins was detected between the control group and the model group, and the difference gradually increased with increases in the time of exposure to cigarette smoke (Fig. 6). The transplantation of BMSCs reduced apoptosis in lung tissue. The pBABE-BMSC group exhibited reduced expression of cleaved caspase-8 ($p < 0.01$), cleaved caspase-3 ($p > 0.05$) and cleaved PARP-1 ($p > 0.05$) in the third month (Fig. 6-C) compared with the model group, and no significant difference was found between the two groups in the first and second months (Fig. 6-A, B). More significantly, the difference in the expression of apoptotic proteins between the CXCR4-BMSC group and the model group was greater. The difference in the expression of cleaved caspase-8 between the two groups was significant ($p < 0.05$, Fig. 6-B) in the second month, but no significant difference in the expression of cleaved caspase-3 was detected (Fig. 6-B). In the third month, the CXCR4-BMSC group exhibited significantly lower protein levels of cleaved caspase-8 ($p < 0.01$, Fig. 6-C), cleaved caspase-3 (Fig. 6-C) and cleaved PARP-1 ($p < 0.05$, Fig. 6-C) than the model group.

4. Discussion

COPD remains a chronic disease with a high mortality rate, and the mortality rate is still increasing yearly due to a lack of effective treatment[10][11][12]. Studies have confirmed that apoptosis is extremely important in the occurrence and development of COPD[2][3], and antiapoptotic therapy is considered a new strategy for COPD treatment. At present, the antiapoptotic effect of BMSCs has been assessed in the treatment of various diseases[34][35][36], and this study further demonstrates the antiapoptotic effect of BMSCs in the progression of COPD.

The cells obtained using the whole bone marrow adherent method have the potential for multidirectional differentiation and can be induced to differentiate into osteoblasts, adipocytes, and chondrocytes. Flow

cytometric assays showed that the surface antigens of the cells conformed to the criteria for BMSCs. The chemokine receptors of BMSCs play an important role in disease treatment, but the expression of chemokine receptors in BMSCs was reduced during the processes of isolation and purification[37]. In this study, CXCR4 overexpression in BMSCs was induced by retroviral transfection.

Smoking is the primary pathogenic factor of COPD, and SD model rats with COPD were constructed by exposure to cigarette smoke in this study. After exposure to cigarette smoke, a significant increase in the MLI was correlated with alveolar enlargement and parenchymal wall destruction, and the destruction of the parenchymal wall increased gradually with increases in the exposure time to cigarette smoke. The TUNEL assay showed that the destruction of alveoli was associated with cell apoptosis. Moreover, cigarette smoke exposure caused DNA fragmentation and resulted in apoptosis; thus, the expression of apoptosis-related proteins in the lung was significantly increased. The analysis of apoptosis-related proteins revealed that cigarette smoke induced cleavage of caspase-8 by TNF-related apoptosis-inducing ligand and that caspase-3 could be cleaved by cleaved caspase-8. Furthermore, we detected DNA breaks in the nucleus, which could be due to increased expression of cleaved PARP-1 protein, and the trend found for the expression of cleaved PARP-1 was similar to the rate of apoptosis in lung tissue determined by TUNEL assays. All of these results showed that apoptosis-related protein expression and DNA fragmentation were increased in the COPD models. Exposure to cigarette smoke could induce alveolar septal rupture, and the alveolar cavity expanded, which could be related to DNA breaks in the nucleus and eventually lead to apoptosis of lung tissue cells.

The transplantation of BMSCs in vivo is often used for the treatment of lung disease, and transplantation via the tail vein is a common transplantation method used with rat models. BMSCs were transplanted in vivo via the tail vein during the process of COPD model generation in SD rats in this study. Histological observations and MLI measurements showed that BMSCs transplanted in vivo via the tail vein reduced alveolar septal rupture and alveolar cavity expansion, and the effects became increasingly obvious with increasing treatment time.

Moreover, the results from a TUNEL assay of lung tissue showed that the transplantation of BMSCs in vivo via the tail vein could reduce apoptosis in lung tissue by reducing the DNA breaks in the nucleus, which could eventually delay the progression of COPD. Cigarette smoke could induce cell apoptosis in lung tissue through various pathways, and the results described above showed that the transplantation of BMSCs in vivo could reduce cell apoptosis, which may be related to reductions in nuclear DNA breakage. To further explore the therapeutic effect of the transplantation of BMSCs in SD model rats with COPD, we detected and compared the expression of apoptosis-related proteins in the lung tissues between the various groups. The analysis of apoptosis-related proteins in the lung tissue in the third month showed that BMSC transplantation could reduce the expression of cleaved PARP-1 and nuclear DNA breakage compared with those in the model group. Moreover, the expression of cleaved caspase-8 and cleaved caspase-3 was substantially reduced in the BMSC transplantation groups compared with the model group. All these results indicated that the transplantation of BMSCs in vivo via the tail vein could

inhibit the exogenous apoptotic pathway to reduce cell apoptosis by decreasing DNA fragmentation in the nucleus, and BMSCs overexpressing CXCR4 yielded better therapeutic outcomes.

Apoptosis in cells can be divided into early apoptosis and advanced apoptosis, and proapoptotic proteins can be activated at the early apoptosis stage[38][39]. The results revealed that BMSCs can inhibit early apoptosis in lung tissue by inhibiting the exogenous apoptotic pathway. The treatment initially yielded no effect, but a clear difference was detected at approximately the third month of therapy. The finding was attributed to the mixture of cigarette smoke that accumulated in the circulatory system during the construction of the apoptosis model, which could impact the therapeutic effect of BMSCs. For example, nicotine interacts with BMSCs via choline receptors and affects BMSC migration, differentiation, and paracrine signaling[40][41][42][43]. After cell transplantation, the exposure to cigarette smoke was continued, which further affected the activity and therapeutic effect of BMSCs. The expression of apoptosis-related proteins in lung tissue did not significantly differ among the groups at the early stage of BMSC transplantation therapy due to the effect of cigarette smoke.

The results of this experiment showed that the transplantation of BMSCs overexpressing CXCR4 protein could significantly inhibit apoptosis during the course of COPD. However, further study will be needed to elucidate the exact mechanism by which BMSCs inhibit apoptosis or reduce alveolar damage. BMSCs transplanted via the tail vein can accumulate in the pulmonary circulatory system and participate in the treatment of lung diseases[44][45]. The local expression of SDF-1 increases after lung tissue damage, and BMSCs overexpressing CXCR4 can be recruited to lung tissue much more easily via the SDF-1/CXCR4 axis. Previous research on the therapeutic effect of BMSCs overexpressing CXCR4 has focused on homing to the site of injury through the CXCR4/SDF-1 axis[27][30][46]. However, some studies have shown that BMSCs overexpressing CXCR4 can exhibit enhanced paracrine effects and inhibit apoptosis by secreting cell growth factors, which is believed to be related to SDF-1-induced CXCR4 internalization[47].

This experiment showed that the transplantation of BMSCs overexpressing CXCR4 protein during COPD model establishment could inhibit apoptosis via extrinsic pathways and thereby delay the progression of COPD. However, the underlying antiapoptotic mechanisms of BMSCs overexpressing CXCR4 need to be further elucidated.

Declarations

Acknowledgments

We would like to thank Huimin Liu for help with manuscript preparation.

Funding

This work was supported in part by the Guangdong Province Financial Technology Research and Development, Promotion and Application Special Fund Project (Yue Cai Gong [2013] No. 401).

Conflicts of Interest

The authors declare that there are no conflicts of interest.

Ethics approval and consent to participate

This experiment was approved by the Ethics Committee of the First Affiliated Hospital of Guangdong Pharmaceutical University, Guangzhou, China (SYXK2017-0124).

Consent to Participate

Not applicable

Consent for Publication

All participants have approved this article to be published.

Availability of data and material

The datasets generated and analyzed during the current study are available from the corresponding author upon reasonable request.

Code availability

Not applicable

Authors' contributions

Jiansheng GAO contributed to the conception and design of the study, the provision of study materials, the collection, analysis and interpretation of the data, and the writing of the manuscript. Yuli Liang contributed to the provision of study materials. Jiabao Chen and Huihui Shen contributed to the data collection and analysis. Hua Liu contributed to the writing of the manuscript, specifically its review and editing, project administration, funding acquisition, and supervision. All the authors read and approved the final manuscript.

References

1. Safitri, W., Martini, S., Artanti, K. D., & Li, C. Y. (2021). Smoking from a Younger Age Is the Dominant Factor in the Incidence of Chronic Obstructive Pulmonary Disease: Case-Control Study. Int J Environ Res Public Health, 18(11). 10.3390/ijerph18116047
2. Gogebakan, B., Bayraktar, R., Ulaslı, M., Oztuzcu, S., Tasdemir, D., & Bayram, H. (2014). The role of bronchial epithelial cell apoptosis in the pathogenesis of COPD. Mol Biol Rep, 41(8), 5321-5327. 10.1007/s11033-014-3403-3

3. Aoshiba, K., Zhou, F., Tsuji, T., & Nagai, A. (2012). DNA damage as a molecular link in the pathogenesis of COPD in smokers. Eur Respir J, 39(6), 1368-1376. 10.1183/09031936.00050211
4. Nitta, N. A., Sato, T., Komura, M., Yoshikawa, H., Suzuki, Y., Mitsui, A., . . . Takahashi, K. (2022). Exposure to the heated tobacco product IQOS generates apoptosis-mediated pulmonary emphysema in murine lungs. Am J Physiol Lung Cell Mol Physiol. 10.1152/ajplung.00215.2021
5. Sun, X., Feng, X., Zheng, D., Li, A., Li, C., Li, S., & Zhao, Z. (2019). Ergosterol attenuates cigarette smoke extract-induced COPD by modulating inflammation, oxidative stress and apoptosis in vitro and in vivo. Clin Sci (Lond), 133(13), 1523-1536. 10.1042/cs20190331
6. Paschalaki, K., Rossios, C., Pericleous, C., MacLeod, M., Rothery, S., Donaldson, G. C., . . . Barnes, P. J. (2022). Inhaled corticosteroids reduce senescence in endothelial progenitor cells from patients with COPD. Thorax. 10.1136/thoraxjnl-2020-216807
7. Zhou, Q., Zhang, L., Sun, Y., Xie, M., & Lin, J. (2020). Clinical value of N-acetylcysteine combined with terbutaline sulfate in elderly patients with chronic obstructive pulmonary disease and its effect on apoptosis/anti-apoptosis mechanism. Ann Palliat Med, 9(5), 3393-3401. 10.21037/apm-20-1605
8. Hodge, S., Hodge, G., Holmes, M., & Reynolds, P. N. (2005). Increased airway epithelial and T-cell apoptosis in COPD remains despite smoking cessation. Eur Respir J, 25(3), 447-454. 10.1183/09031936.05.00077604
9. Strulovici-Barel, Y., Staudt, M. R., Krause, A., Gordon, C., Tilley, A. E., Harvey, B. G., . . . Crystal, R. G. (2016). Persistence of circulating endothelial microparticles in COPD despite smoking cessation. Thorax, 71(12), 1137-1144. 10.1136/thoraxjnl-2015-208274
10. Adeloye, D., Chua, S., Lee, C., Basquill, C., Papana, A., Theodoratou, E., . . . Rudan, I. (2015). Global and regional estimates of COPD prevalence: Systematic review and meta-analysis. Journal of global health, 5(2), 020415. 10.7189/jogh.05-020415
11. Rabe, K., Hurd, S., Anzueto, A., Barnes, P., Buist, S., Calverley, P., . . . Zielinski, J. (2007). Global strategy for the diagnosis, management, and prevention of chronic obstructive pulmonary disease: GOLD executive summary. American journal of respiratory and critical care medicine, 176(6), 532-555. 10.1164/rccm.200703-456SO
12. Ferraro, M., Di Vincenzo, S., Dino, P., Bucchieri, S., Cipollina, C., Gjomarkaj, M., & Pace, E. (2019). Budesonide, Aclidinium and Formoterol in combination limit inflammaging processes in bronchial epithelial cells exposed to cigarette smoke. Experimental gerontology, 118, 78-87. 10.1016/j.exger.2019.01.016
13. Teng, C., Jeng, L., & Shyu, W. (2018). Role of Insulin-like Growth Factor 1 Receptor Signaling in Stem Cell Stemness and Therapeutic Efficacy. Cell transplantation, 27(9), 1313-1319. 10.1177/0963689718779777
14. El Haddad, N., Heathcote, D., Moore, R., Yang, S., Azzi, J., Mfarrej, B., . . . Abdi, R. (2011). Mesenchymal stem cells express serine protease inhibitor to evade the host immune response. Blood, 117(4), 1176-1183. 10.1182/blood-2010-06-287979

15. Guan, R., Yao, H., Li, Z., Qian, J., Yuan, L., Cai, Z., . . . Lu, W. (2021). Sodium tanshinone IIA sulfonate attenuates cigarette smoke extract-induced mitochondrial dysfunction, oxidative stress and apoptosis in alveolar epithelial cells by enhancing SIRT1 pathway. Toxicological sciences : an official journal of the Society of Toxicology. 10.1093/toxsci/kfab087
16. Yang, S., Wu, H., Zhao, J., Wu, X., Zhao, J., Ning, Q., . . . Xie, J. (2014). Feasibility of 8-OHdG formation and hOGG1 induction in PBMCs for assessing oxidative DNA damage in the lung of COPD patients. Respirology (Carlton, Vic.), 19(8), 1183-1190. 10.1111/resp.12378
17. English, K., Ryan, J., Tobin, L., Murphy, M., Barry, F., & Mahon, B. (2009). Cell contact, prostaglandin E(2) and transforming growth factor beta 1 play non-redundant roles in human mesenchymal stem cell induction of CD4+CD25(High) forkhead box P3+ regulatory T cells. Clinical and experimental immunology, 156(1), 149-160. 10.1111/j.1365-2249.2009.03874.x
18. Hyvärinen, K., Holopainen, M., Skirdenko, V., Ruhanen, H., Lehenkari, P., Korhonen, M., . . . Kerkelä, E. (2018). Mesenchymal Stromal Cells and Their Extracellular Vesicles Enhance the Anti-Inflammatory Phenotype of Regulatory Macrophages by Downregulating the Production of Interleukin (IL)-23 and IL-22. Frontiers in immunology, 9, 771. 10.3389/fimmu.2018.00771
19. Lim, J., Ryu, D., Lee, S., Park, G., & Min, C. (2017). Mesenchymal Stem Cells (MSCs) Attenuate Cutaneous Sclerodermatous Graft-Versus-Host Disease (Scl-GVHD) through Inhibition of Immune Cell Infiltration in a Mouse Model. The Journal of investigative dermatology, 137(9), 1895-1904. 10.1016/j.jid.2017.02.986
20. Gu, Y., Zhang, Y., Bi, Y., Liu, J., Tan, B., Gong, M., . . . Chen, J. (2015). Mesenchymal stem cells suppress neuronal apoptosis and decrease IL-10 release via the TLR2/NFκB pathway in rats with hypoxic-ischemic brain damage. Molecular brain, 8(1), 65. 10.1186/s13041-015-0157-3
21. Rehman, J., Traktuev, D., Li, J., Merfeld-Clauss, S., Temm-Grove, C., Bovenkerk, J., . . . March, K. (2004). Secretion of angiogenic and antiapoptotic factors by human adipose stromal cells. Circulation, 109(10), 1292-1298. 10.1161/01.Cir.0000121425.42966.F1
22. Gong, H., Cheng, W., & Wang, Y. (2019). Tumor necrosis factor-related apoptosis-inducing ligand inhibits the growth and aggressiveness of colon carcinoma via the exogenous apoptosis signaling pathway. Experimental and therapeutic medicine, 17(1), 41-50. 10.3892/etm.2018.6901
23. Huang, X., Ou, C., Shu, Y., Wang, Y., Gong, S., Luo, R., . . . Gong, C. (2021). A self-sustained nanoplatform reverses TRAIL-resistance of pancreatic cancer through coactivating of exogenous and endogenous apoptotic pathway. Biomaterials, 272, 120795. 10.1016/j.biomaterials.2021.120795
24. Vagima, Y., Lapid, K., Kollet, O., Goichberg, P., Alon, R., & Lapidot, T. (2011). Pathways implicated in stem cell migration: the SDF-1/CXCR4 axis. Methods in molecular biology (Clifton, N.J.), 750, 277-289. 10.1007/978-1-61779-145-1_19
25. Saito, Y., Shimada, M., Utsunomiya, T., Ikemoto, T., Yamada, S., Morine, Y., . . . Takasu, C. (2014). Homing effect of adipose-derived stem cells to the injured liver: the shift of stromal cell-derived

factor 1 expressions. Journal of hepato-biliary-pancreatic sciences, 21(12), 873-880. 10.1002/jhbp.147

26. Wang, Y., Fu, W., Zhang, S., He, X., Liu, Z., Gao, D., & Xu, T. (2014). CXCR-7 receptor promotes SDF-1α-induced migration of bone marrow mesenchymal stem cells in the transient cerebral ischemia/reperfusion rat hippocampus. Brain research, 1575, 78-86. 10.1016/j.brainres.2014.05.035
27. Wang, Z., Wang, Y., Wang, Z., Gutkind, J., Wang, Z., Wang, F., . . . Chen, X. (2015). Engineered mesenchymal stem cells with enhanced tropism and paracrine secretion of cytokines and growth factors to treat traumatic brain injury. Stem cells (Dayton, Ohio), 33(2), 456-467. 10.1002/stem.1878
28. Shahzad, U., Li, G., Zhang, Y., Li, R., Rao, V., & Yau, T. (2015). Transmyocardial Revascularization Enhances Bone Marrow Stem Cell Engraftment in Infarcted Hearts Through SCF-C-kit and SDF-1-CXCR4 Signaling Axes. Stem cell reviews and reports, 11(2), 332-346. 10.1007/s12015-014-9571-7
29. Yang, J., Zhang, N., Wang, H., Gao, P., Yang, Q., & Wen, Q. (2015). CXCR4 receptor overexpression in mesenchymal stem cells facilitates treatment of acute lung injury in rats. The Journal of biological chemistry, 290(4), 1994-2006. 10.1074/jbc.M114.605063
30. Chen, H., Zhu, H., Chu, Y., Xu, F., Liu, Y., Tang, B., . . . Zhang, Y. (2014). [Construction of mouse VCAM-1 expression vector and establishment of stably transfected MSC line C3H10T1/2]. Zhongguo shi yan xue ye xue za zhi, 22(5), 1396-1401. 10.7534/j.issn.1009-2137.2014.05.041
31. Li, Y., Li, S., Li, J., Deng, L., Tian, Y., Jiang, S., . . . Wang, Y. (2012). A rat model for stable chronic obstructive pulmonary disease induced by cigarette smoke inhalation and repetitive bacterial infection. Biological & pharmaceutical bulletin, 35(10), 1752-1760. 10.1248/bpb.b12-00407
32. Lin, J., Xu, F., Wang, G., Kong, L., Luo, Q., Lv, Y., . . . Dong, J. (2016). Paeoniflorin Attenuated Oxidative Stress in Rat COPD Model Induced by Cigarette Smoke. Evidence-based complementary and alternative medicine : eCAM, 2016, 1698379. 10.1155/2016/1698379
33. Zhao, Q., Hao, C., Wei, J., Huang, R., Li, C., & Yao, W. (2021). Bone marrow-derived mesenchymal stem cells attenuate silica-induced pulmonary fibrosis by inhibiting apoptosis and pyroptosis but not autophagy in rats. Ecotoxicol Environ Saf, 216, 112181. 10.1016/j.ecoenv.2021.112181
34. Xu, T. B., Li, L., Luo, X. D., & Lin, H. (2017). BMSCs protect against liver injury via suppressing hepatocyte apoptosis and activating TGF-β1/Bax singling pathway. Biomed Pharmacother, 96, 1395-1402. 10.1016/j.biopha.2017.11.023
35. Zhang, C. S., Shao, K., Liu, C. W., Li, C. J., & Yu, B. T. (2019). Hypoxic preconditioning BMSCs-exosomes inhibit cardiomyocyte apoptosis after acute myocardial infarction by upregulating microRNA-24. Eur Rev Med Pharmacol Sci, 23(15), 6691-6699. 10.26355/eurrev_201908_18560
36. Rombouts, W., & Ploemacher, R. (2003). Primary murine MSC show highly efficient homing to the bone marrow but lose homing ability following culture. Leukemia, 17(1), 160-170. 10.1038/sj.leu.2402763
37. Duncan-Lewis, C., Hartenian, E., King, V., & Glaunsinger, B. (2021). Cytoplasmic mRNA decay represses RNA polymerase II transcription during early apoptosis. eLife, 10. 10.7554/eLife.58342

38. Khalil, C., Chahine, J., Haykal, T., Al Hageh, C., Rizk, S., & Khnayzer, R. (2021). E-cigarette aerosol induced cytotoxicity, DNA damages and late apoptosis in dynamically exposed A549 cells. Chemosphere, 263, 127874. 10.1016/j.chemosphere.2020.127874
39. Benowitz, N., Hukkanen, J., & Jacob, P. (2009). Nicotine chemistry, metabolism, kinetics and biomarkers. Handbook of experimental pharmacology(192), 29-60. 10.1007/978-3-540-69248-5_2
40. Zeng, H., Qin, Y., Chen, H., Bu, Q., Li, Y., Zhong, Q., . . . Liu, G. (2014). Effects of nicotine on proliferation and survival in human umbilical cord mesenchymal stem cells. Journal of biochemical and molecular toxicology, 28(4), 181-189. 10.1002/jbt.21551
41. Zhou, Y., Gan, Y., & Taylor, H. (2011). Cigarette smoke inhibits recruitment of bone-marrow-derived stem cells to the uterus. Reproductive toxicology (Elmsford, N.Y.), 31(2), 123-127. 10.1016/j.reprotox.2010.10.007
42. Wahl, E., Schenck, T., Machens, H., & Egaña, J. (2016). Acute stimulation of mesenchymal stem cells with cigarette smoke extract affects their migration, differentiation, and paracrine potential. Scientific reports, 6, 22957. 10.1038/srep22957
43. Lee, R., Pulin, A., Seo, M., Kota, D., Ylostalo, J., Larson, B., . . . Prockop, D. (2009). Intravenous hMSCs improve myocardial infarction in mice because cells embolized in lung are activated to secrete the anti-inflammatory protein TSG-6. Cell stem cell, 5(1), 54-63. 10.1016/j.stem.2009.05.003
44. Yang, Y., Li, Y., Wang, Y., Ruan, G., Tian, C., Wang, Q., . . . Pan, X. (2021). The effects of BMMSC treatment on lung tissue degeneration in elderly macaques. Stem cell research & therapy, 12(1), 156. 10.1186/s13287-021-02201-3
45. Shahzad, U., Li, G., Zhang, Y., Li, R., Rao, V., & Yau, T. (2015). Transmyocardial Revascularization Enhances Bone Marrow Stem Cell Engraftment in Infarcted Hearts Through SCF-C-kit and SDF-1-CXCR4 Signaling Axes. Stem cell reviews and reports, 11(2), 332-346. 10.1007/s12015-014-9571-7
46. Wu, S., Li, Y., Huang, W., Cai, W., Liang, J., Paul, C., . . . Wang, Y. (2017). Paracrine effect of CXCR4-overexpressing mesenchymal stem cells on ischemic heart injury. Cell biochemistry and function, 35(2), 113-123. 10.1002/cbf.3254

Figures

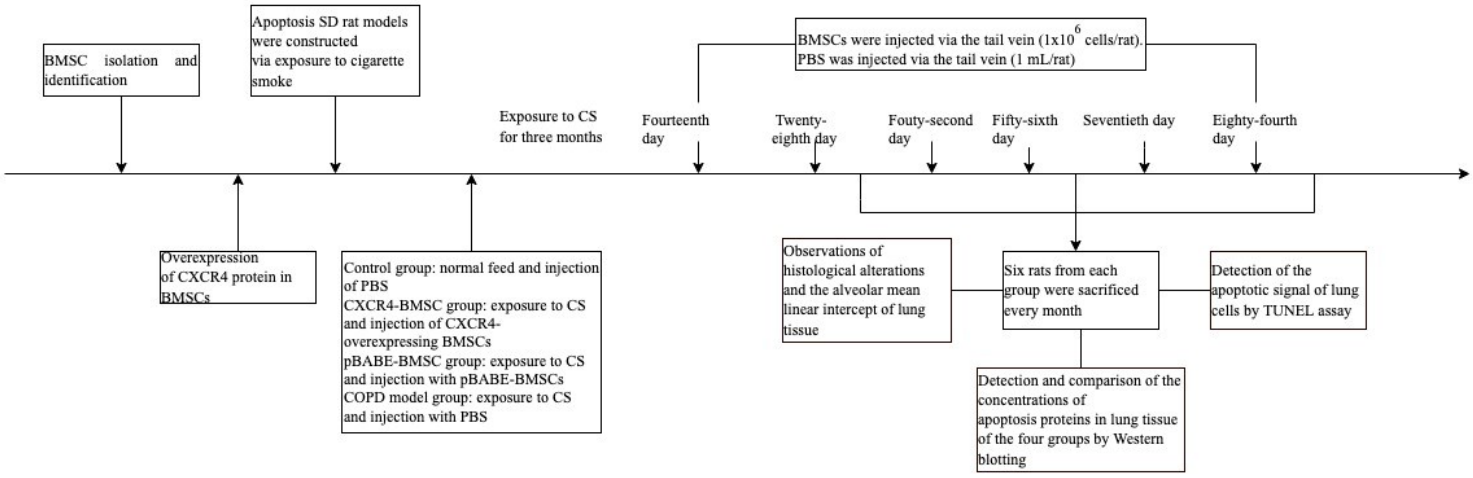

Figure 1

Legend not included with this version

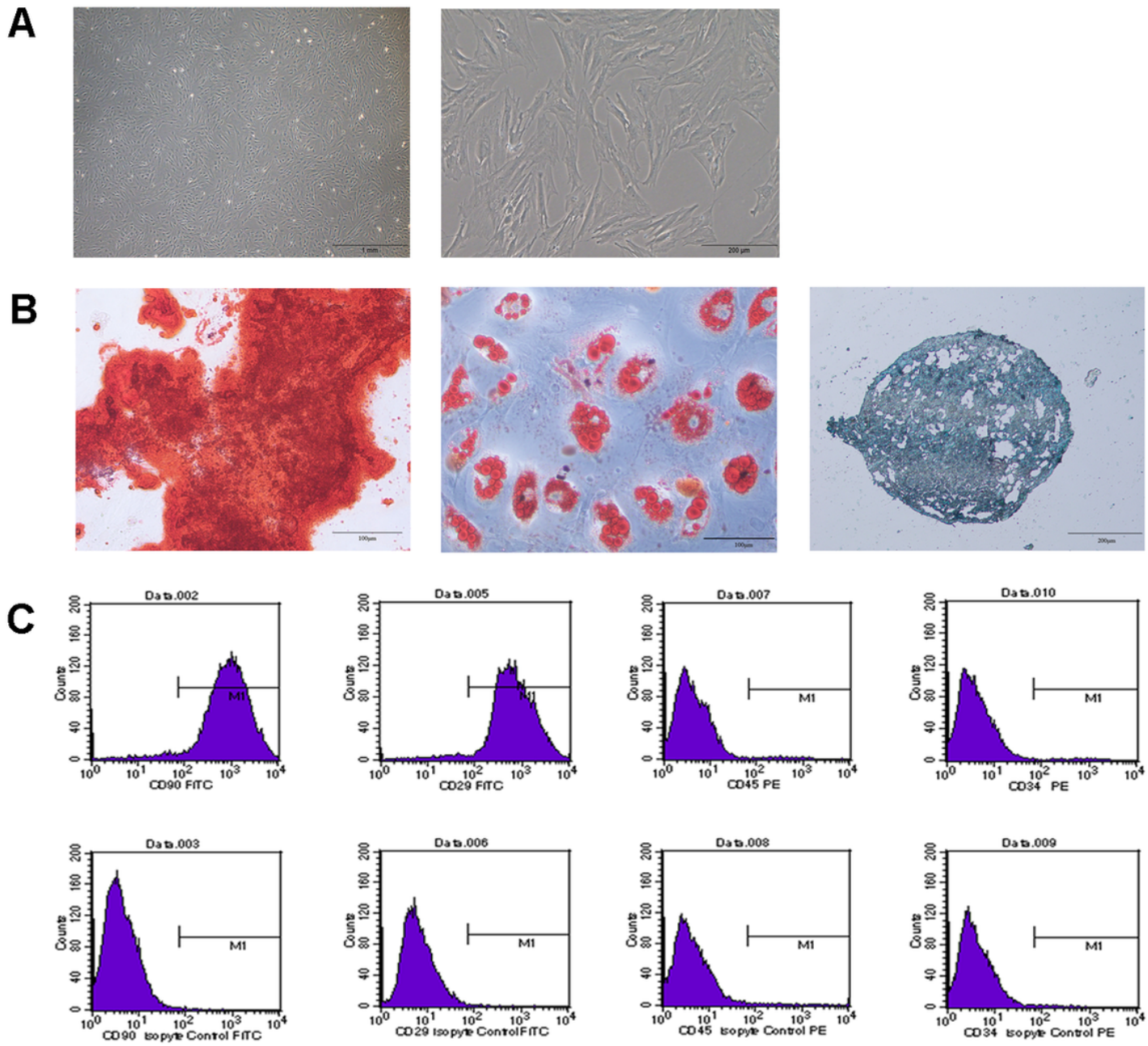

Figure 2

Results from the identification of bone marrow mesenchymal stem cells

A: After separation and purification, the stem cells exhibited a typical spindle shape.

B: The cells could be differentiated into osteoblasts , adipocytes and chondrocytes.

C: The cellular immune phenotype matched the characteristics of bone marrow mesenchymal stem cells.

A

Group		CXCR4	18s	ΔCt	ΔΔCt	RQ
	Ct1	34.34	9.09	25.19	-0.06	1.04
pBABE-	Ct2	34.98	9.18	25.83	0.58	0.67
BMSCs	Ct3	33.88	9.19	24.73	-0.52	1.43
	Ct1	32.21	9.01	23.17	-2.08	4.22
CXCR4-	Ct2	32.02	9.08	22.98	-2.27	4.81
BMSCs	Ct3	31.87	9.03	22.83	-2.42	5.34

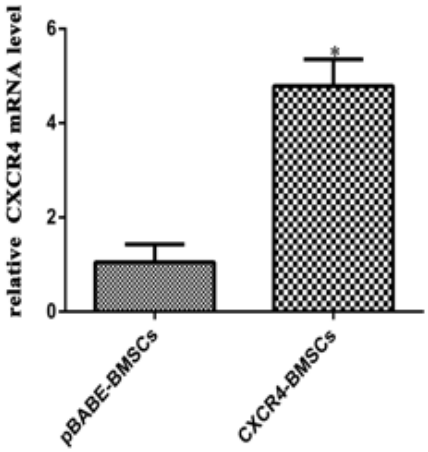

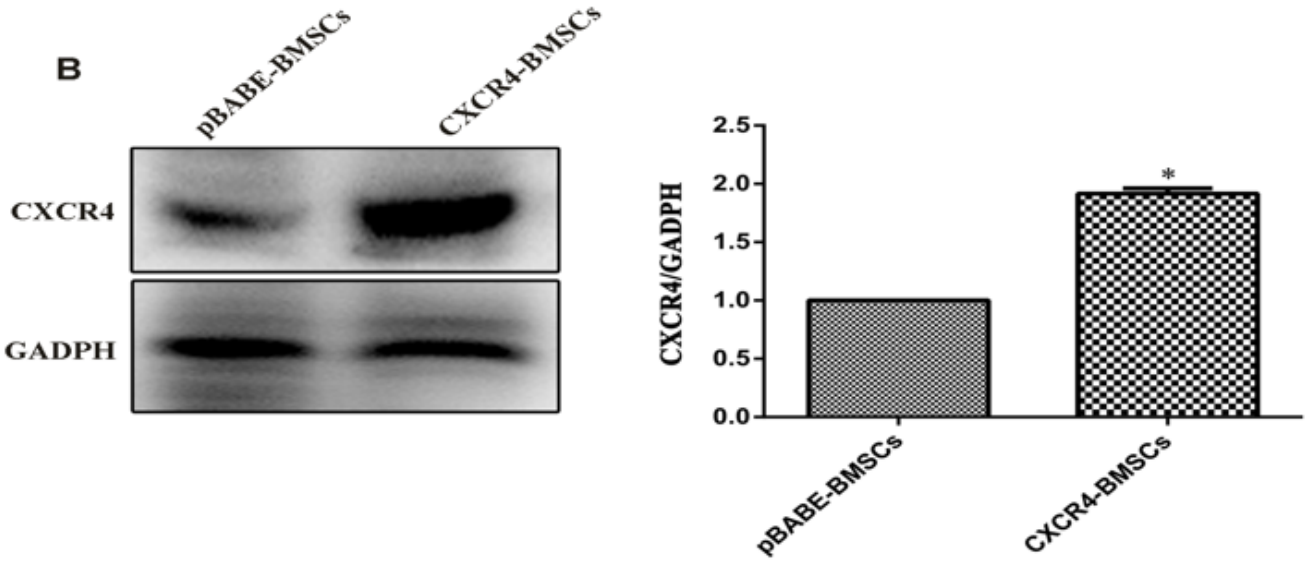

Figure 3

Establishment of stable CXCR4-overexpressing BMSCs

After retrovirus transfection, the CXCR4 mRNA level in the CXCR4-BMSCs was significantly increased (Figure 3-A, *p<0.001), and CXCR4 protein was stably expressed (Figure 3-B, *p<0.01).

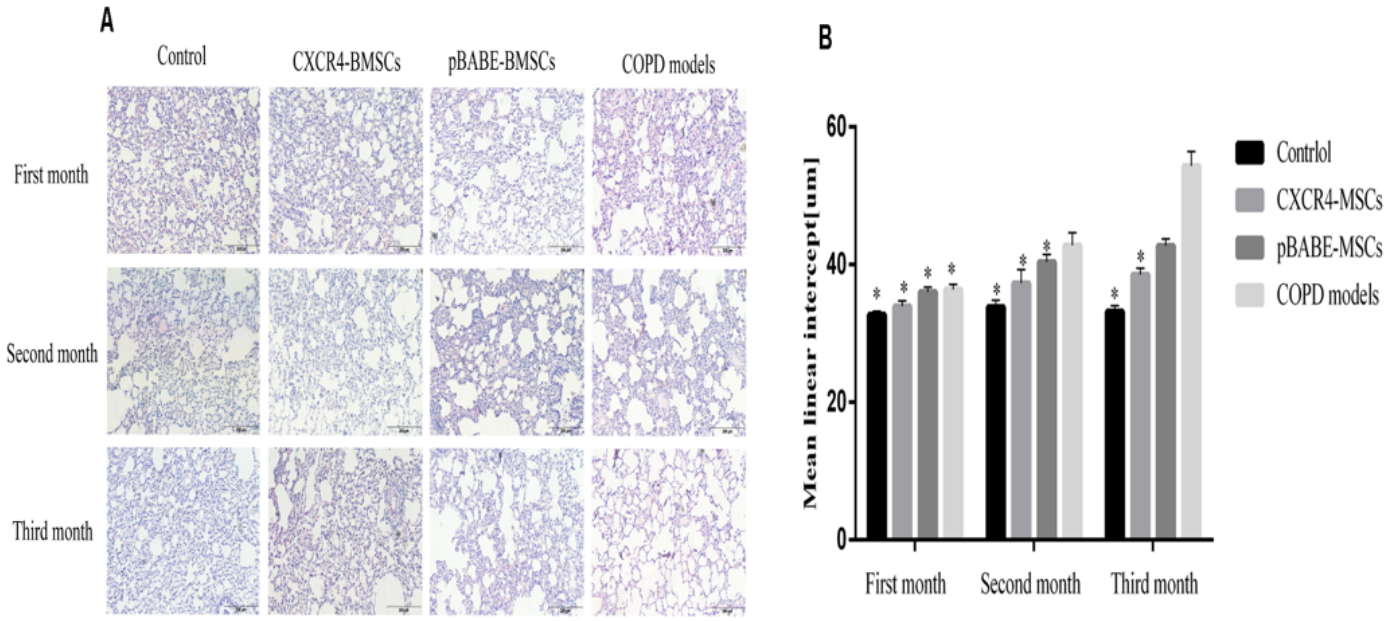

Figure 4

Effects of CXCR4-overexpressing BMSC transplantation on lung tissue protection in COPD rat models

In the COPD rat models, the CXCR4-overexpressing BMSCs slowed lung tissue destruction (Figure 4-A), and the alveolar MLI in the third month of the CXCR4-BMSC group was significantly lower than that of the model group (*p<0.05, **p<0.01).

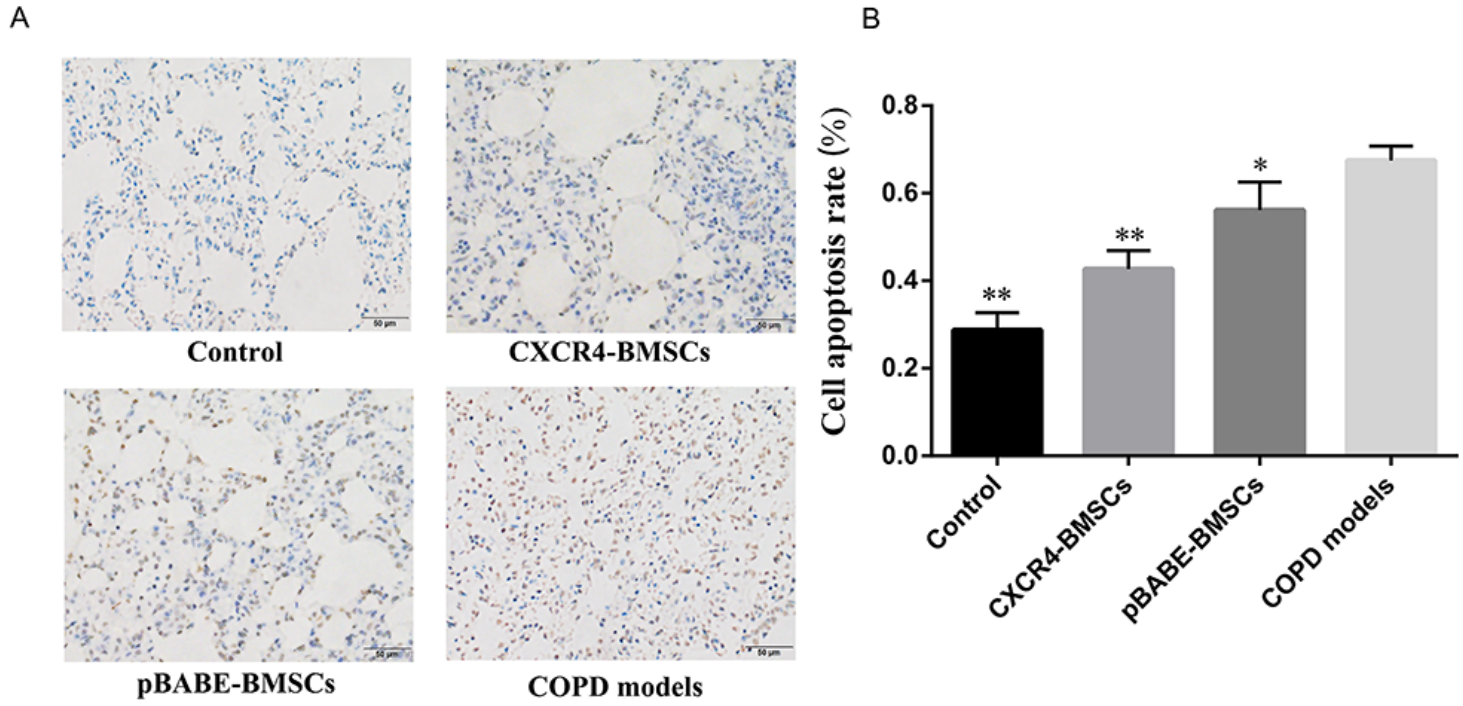

Figure 5

CXCR4-overexpressing BMSC transplantation reduced apoptosis in the lungs of COPD rat models

Apoptotic cells were stained brown in lung tissue (Figure 5-A). The data are presented as the means ± SDs. Significant differences are indicated (**p<0.01 and *p<0.05 versus the control group, pBABE-BMSC group, CXCR4-BMSC group and COPD model group; Figure 5-B).

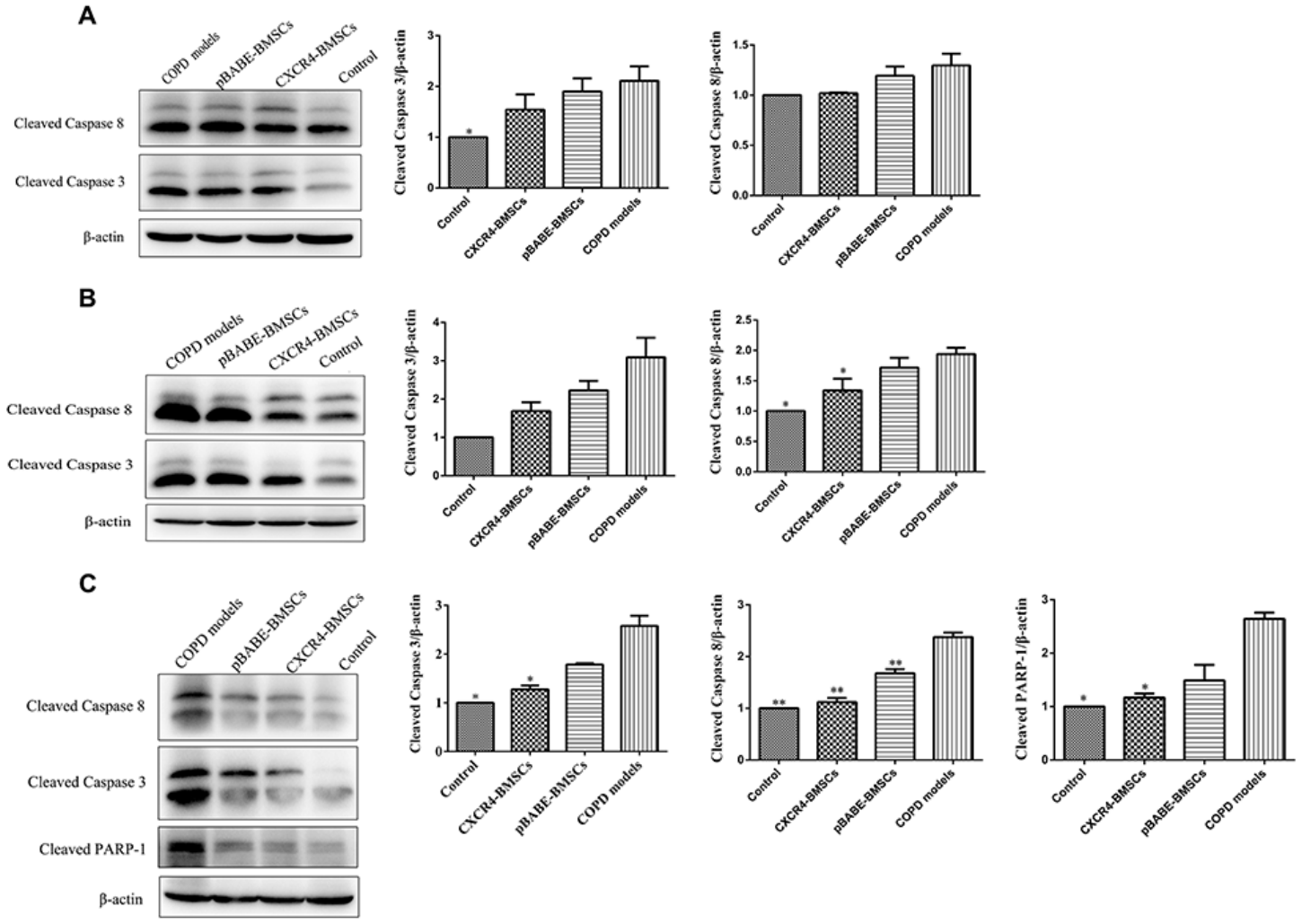

Figure 6

CXCR4-overexpressing BMSC transplantation reduced the expression of apoptosis-related proteins in the lung tissue of COPD rat models

Western blotting revealed a marked reduction in the expression of apoptotic proteins in the BMSC-treated rats, particularly in the CXCR4-overexpressing BMSC-treated rats. The dynamics of the expression of apoptosis-related proteins in the lung tissue during construction of the COPD rat models were observed. The expression of apoptosis-related proteins in the first, second and third months was detected, and the results showed that the CXCR4-overexpressing BMSCs could significantly inhibit the exogenous apoptosis pathway to reduce the apoptosis in lung tissue, as shown by the reduced expression of cleaved caspase-8, cleaved caspase-3 and cleaved PARP-1. The data are presented as the means ± SDs.

Statistically significant differences are indicated (**p<0.01 and *p<0.05 versus the control group, pBABE-BMSC group, CXCR4-BMSC group and model group).

Supplementary Files

This is a list of supplementary files associated with this preprint. Click to download.

- GA.png